Am J Cancer Res 2020;10(2):507-522
www.ajcr.us /ISSN:2156-6976/ajcr0096526

Original Article

Trifluridine selectively inhibits cell growth and induces cell apoptosis of triple-negative breast cancer

Juan Li[1,2], Jie Liu[1,2], Riqi Wang[1,2], He Chen[1,2], Cui Li[1,2], Minggang Zhao[1,2], Fang He[1,2], Yaochun Wang[1,2], Peijun Liu[1,2]

[1]*Center for Translational Medicine,* [2]*Key Laboratory for Tumor Precision Medicine of Shaanxi Province, The First Affiliated Hospital of Xi'an Jiaotong University, Xi'an, Shaanxi, PR China*

Received May 5, 2019; Accepted January 10, 2020; Epub February 1, 2020; Published February 15, 2020

Abstract: Triple-negative breast cancer (TNBC) is one of the most aggressive cancers with a high rate of recurrence and metastasis. Trifluridine (TFT) is a thymidine analog to target thymidylate synthase (TS) and has potent ant-herpes simplex virus activity. However, little is known whether and how TFT treatment can modulate the growth of TNBC. In this study, we found that treatment with TFT selectively inhibited the proliferation of TNBC cells and triggered their apoptosis. TFT treatment significantly up-regulatd the expression of G1 phase inhibitor p21 and p27, and pro-apoptotic factor γ-H2AX, Bax and cleaved caspase-7 in TNBC cells. TFT treatment significantly down-regulated the expression of proliferating cell nuclear antigen (PCNA), minichromosome maintenance component 7 (MCM7) and anti-apoptotic Bcl-2 in TNBC cells. TFT treatment significantly mitigated the growth of implanted mouse TNBC in vivo, associated with increased expression of γ-H2AX and cleaved caspase-7 in mouse TNBC tumors. TS expression was up-regulated in breast cancer, particularly in TNBC tissues, and up-regulated TS expression was significantly associated with a shorter overall survival and disease free survival in TNBC patients. TS silencing selectively decreased the proliferation of TNBC cells, but did not trigger their apoptosis. Treatment with TFT induced DNA double strand break (DSB) and damages in TNBC cells. Collectively, TFT selectively inhibited the growth of TNBC by inducing chromosome instability and inhibiting thymidine synthase. Therefore, TFT may be valuable for the intervention of TNBC.

Keywords: Trifluridine, triple-negative breast cancer, proliferation, cell apoptosis, chromosome instability

Introduction

Triple negative breast cancer (TNBC) is a very aggressive type of cancer and accounts for 15-20% of total cases of breast cancers [1, 2]. TNBC is associated with poor prognosis because of its high recurrence and distant metastasis [3]. Due to the lack of estrogen receptor (ER), progesterone receptor (PR) and human epithermal growth factor receptor 2 (HER2) expression, TNBC is commonly insensitive to targeted and endocrinal hormone therapies [4]. Most patients with TNBC usually depend on surgical resection, chemotherapies and radiotherapies. However, the available therapeutic strategies usually have severe side-effects due to their non-selective nature. Therefore, discovery of new drugs will be of great significance in management of patients with TNBC.

Trifluridine (TFT) is a thymidine analog and has potent anti-herpes simplex virus activity because it can incorporate into virus DNA to limit virus DNA replication [5]. Previous studies have shown that the single phosphorylation form of TFT can inhibit the activity of thymidylate synthase (TS) [6, 7]. Further studies reveal that the triphosphorylation form of TFT can incorporate into DNA and cause DNA damage [8, 9]. It has been shown that up-regulated TS expression is associated with poor prognosis of several types of cancers and inhibition of TS attenuates the growth of colon, lung and other types of cancer cells [10-12]. TFT can also induce DNA double strand break (DSB) and trigger cancer cell apoptosis [13]. However, little is known whether TFT can inhibit the proliferation of TNBC cells, what levels of TS expression are in TNBC and how TS expression is associated with the prognosis of TNBC.

In this study, we investigated the effect of TFT treatment on the proliferation and apoptosis of

different types of breast cancer cells and tested the efficacy of TFT in inhibiting the growth of implanted mouse TNBC tumors in mice. Furthermore, we examined the expression of TS and its association with clinical measures in database and breast cancer patients. Moreover, we examined the effect of TS silencing on the proliferation and apoptosis of breast cancer cells. Our data indicated that treatment with TFT selectively inhibited the proliferation of TNBC cells and induced their apoptosis. Treatment with TFT induced chromosome instability of TNBC cells. Furthermore, up-regulated TS expression was associated with poor prognosis of TNBC and TS silencing inhibited the proliferation of TNBC cells. Therefore, TFT may be a valuable candidate for the intervention of TNBC.

Materials and methods

Cells

Human mammary epithelial MCF-10A, luminal A subtype of breast cancer cells MCF-7, TNBC subtype of breast cancer cells MDA-MB-231, BT-549 and Hs578T and mouse breast carcinoma 4T1 cells were obtained from American Type Culture Collection (ATCC, VA, USA). MCF-10A were cultured in DMEM/F12 medium (Hyclone) supplemented with 5% horse serum (Hyclone), 1% penicillin/streptomycin (Hyclone), 0.5% μg/ml hydrocortisone (Sigma, H-0888), 10 μg/ml insulin (Sigma, I-1882) and 20 ng/ml recombinant human EGF (Peprotech, 100-15). MCF-7, MDA-MB-231, BT-549, Hs578T and 4T1 cells were cultured in DMEM medium (Hyclone) supplemented with 10% FBS (Hyclone). All cell cultures were maintained at 37°C in a humidified atmosphere containing 5% CO_2.

Transfection and transduction

MCF-7, MDA-MB-231 and BT-549 cells were transfected with control scramble or TS-specific siRNAs (GenePharma, Shanghai, China) using lipofectamine 3000 (Invitrogen), according to the manufacturer's instruction. The sequences of TS-specific siRNAs were siTS-1 5'CCU GAA GCC AGG UGA CUU UTT3'; siTS-2 5'CCA ACU GCA AAG AGU GAU UTT3'. MDA-MB-231 cells were transduced with control lentivirus or lentivirus for expression of TS-shRNA (Genechem, Shanghai, China) to generate stably TS-silencing MDA-MB-231.

Cell viability

The cytotoxic effect of individual drugs was determined by the 3-[4,5-dimethylthiazol-2-yl]-2,5-diphenyltetrazolium bromide (MTT) assay (Thermo Fisher-Scientific, Waltham, USA). Briefly, MDA-MB-231 cells (1×10^4 cells/well) were cultured in 96-well plates and treated in triplicate with, or without, vehicle 2% DMSO or individual drugs at 5 μM in the FDA-approved drug library (Selleck company, TX, USA) for 48 h. During the last 4 h culture, individual wells of cells were exposed to 20 μl of MTT solution (20 mg/ml) and the generated formazan was dissolved in DMSO, followed by measuring absorbance at 490 nm in a microplate reader. In addition, the impact of TFT on cell viability was assessed by MTT assays. Individual types of cells (1×10^4 cells/well) were cultured in DMEM medium in 96-well plates overnight and treated in triplicate with vehicle or different concentrations (5-20 μM) of TFT (Selleck, USA) for 24-72 h.

Colony formation assay

The impact of TFT on the clonogenicity of TNBC cells was examined by colony formation assay. Briefly, the different types of cells (5×10^3 cells/well) were cultured in 6-well plates in the presence or absence of 10 or 20 μM TFT for 10-12 days. The cells were stained with 0.5% crystal violet solution. The numbers of colonies were counted in a blinded manner.

Flow cytometry

The effect of TFT on cell proliferation was analyzed by flow cytometry. Briefly, individual types of cells were labeled with CFSE (5,6-carboxyfluorescein diacetate, succinimidyl ester). After being washed, the cells (2×10^5 cells/well) were cultured in 6-well plates overnight and treated with vehicle or 10 or 20 μM TFT for 48 h. The proliferation of breast cancer cells was analyzed by flow cytometry.

Similarly, the effect of TFT on cell apoptosis was determined by flow cytometry. Briefly, individual types of cells were treated vehicle or 10 or 20 μM TFT for 48 h. The cells were stained with FITC-Annexin V and 7-ADD (7-amino-actinomycin D). The frequency of apoptotic cells was determined by flow cytometry.

Table 1. The demographic and clinical characteristics of breast cancer patients

Parameter	No. of patients (%)
Age (years)	
<60	32 (57)
≥60	24 (43)
T-stage	
cT1	16 (29)
cT2	35 (62)
cT3-4	5 (9)
N-stage	
N0	39 (70)
Nx	17 (30)
M-stage	
M0	56 (100)
M1	0 (0)
TNM phase	
I	11 (20)
II	30 (53)
III	15 (27)
Classification	
Luminal A	36 (64)
HER2+	5 (9)
TNBC	15 (27)
ER status	
negative	20 (36)
positive	36 (64)
PR status	
negative	23 (41)
positive	33 (59)
HER2 status	
negative	51 (91)
positive	5 (9)

Abbreviations: TNM = tumor, node, metastases; ER = estrogen receptor; HER = human epidermal growth factor receptor; PR = progesterone receptor.

Chromosomal instability assays

The effect of TFT on chromosomal stability was tested, as described previously [14]. Briefly, MCF-10A, MCF-7, MDA-MB-231 and BT549 cells were treated with vehicle or 10 μM TFT for 72 h. The cells were treated with 0.5%-1% of colchicine at 37°C for 4 h, 0.56 M KCl for 15 min at room temperature. The cells were fixed in 3:1 vol/vol methanol/acetic acid and dropped onto glass-slides, followed by drying for 2 h at 65°C. The cells were digested with 0.05%-0.1% trypsin and stained with Giemsa staining solution, followed by photoimaging in a chromosome karyotype analyzer (ZEISS, Oberkochen, Germany).

Immunofluorescence

MCF-10A, MCF-7, MDA-MB-231 and BT549 cells were grown on coverslips and treated with vehicle or 20 μM TFT for 72 h. The cells were fixed with 4% paraformaldehyde for 10 min and permeabilized with 0.1% Triton-X100 for 10 min, followed by blocked with 5% BSA or 10% horse sera in TBST for 1 h. After being washed with TBST, the cells were probed with primary antibodies (1:100) against γ-H2AX overnight at 4°C. The bound antibodies were detected with Alexa Fluor 488-labeled secondary antibodies (Invitrogen) and photoimaged under a fluorescent microscope (Leica TCS SP5 II, Leica, Wetzlar, Germany).

Comet assays

The impact of TFT treatment on DSB in breast cancer cells was determined by alkaline comet assay using a Single Cell Gel Electrophoresis Assay Kit (Trevigen, USA) according to the manufacturer's instructions. Briefly, MCF-10A, MCF-7, MDA-MB-231 and BT549 cells were treated with vehicle or 10 μM TFT for 72 h. The cells (100 cell per group) were tested and 50 cells were randomly selected from each group for quantitative analysis, using the CASP1.2.3 beta1 software (Krzysztof Konca, Comet Assay Software Project Lab, http://caspla.com).

Immunohistochemistry staining

Breast cancer tissue array was purchased from Shanghai Xinchao Biobank (Shanghai, China). The tissue array contained 41 surgical para-breast cancer tissue and 56 breast cancer tissues, including 36 luminal A, 5 HER2+ and 15 TNBC tissues, which were obtained from the patients after neo-adjuvant therapies. Their demographic and clinical characteristics are shown in **Table 1**. The tissue sections were deparaffinized, rehydrated and subjected to antigen retrieval using 0.01 M sodium citrate in a microwave. After being blocked with 10% goat sera, the tissue sections were incubated with primary anti-TS antibody (1:300, SC-20528), anti-PCNA antibody (1:200, SC-56, Santa Cruz) and anti-Ki67 antibody (1:500, #12202, Cell Signaling) and at 4°C overnight. After being washed with TBST, the bound antibodies were detected with *horseradish peroxidase* (HRP)-conjugated secondary antibody and stained with 3,3'-diaminobenzidine (DAB), followed by

counterstained with hematoxylin. The sections were photoimaged under a Leica microscope (SCN 400, Mannheim, Germany). Each immunohistochemistry image was scored by a pathologist in three different microscopic fields in a blinded manner. The expression levels of TS were assessed as the percentage of TS+ tumor cells. The percentage of positively stained cells was scored as 0 (<10%), 1 (10-40%), 2 (40-70%) or 3 (>70%). The intensity of immunohistochemistry staining was scored as 0 (negative), 1 (weakly positive), 2 (moderately positive), or 3 (strongly positive).

Immunoblot analysis

Individual groups of cells were lysed in a RIPA buffer and centrifuged. The protein concentrations of each sample were determined by the BCA method. The cell lysate samples (30 μg/lane) were separated by sodium dodecyl sulfate polyacrylamide gel electrophoresis (SDS-PAGE) on 6-12% gels and transferred onto polyvinylidene difluoride (PVDF) membranes (Millipore, Bedford, MA, USA). The membranes were blocked with 5% BSA in TBST and probed with primary anti-MCM7, anti-p27, anti-Bcl2 (Santa Cruz), anti-γ-H2AX (Millipore) and other antibodies (Cell Signaling Technology, Beverly, MA, USA) and visualized by the enhanced chemiluminescence reagent (Cell Signaling Technology).

Mouse model of breast cancer

The animal experiments were approved by the Institutional Animal Care and Use Committee of Xi'an Jiaotong University. Female BALB/C mice at 6 weeks of age were injected with 1×10^6 mouse breast cancer 4T1 cells (ER-, PR-, HER2-) in their fat pad [15]. When tumors reached in 30-40 mm^3, the tumor-bearing mice were randomized and treated with vehicle (H_2O), 75 mg/kg or 150 mg/kg TFT by gavage daily for 10 consecutive days. The growth of implanted tumors was monitored every other day. At the end of the experiment, the tumors were dissected out, imaged and their weights were measured. The Ki67, PCNA and γ-H2AX expression were analyzed by immunohistochemistry and immunofluorescence. Similiarly, NOD/SCID mice at 6 weeks of age were injected with 2×10^7 MM231/shCon or MM231/shTS cells in their fat pad. At the end of the experiment, the tumors were dissected out, imaged and their weights were measured.

Statistical analysis

Data are expressed as mean ± S.E.M, or median ± IQR. The difference of normally distributed data among groups was determined by one way analysis of variance (ANOVA) and post hoc Tukey's test and the difference between groups was analyzed by Student's T test. The difference of skewed data between groups was analyzed by Wilcoxon signed-rank test. The potential correlation between TS expression and clinical measures was analyzed using the GEPIA (Gene Expression Profiling Interactive Analysis) tools, and LinkFinder in LinkedOmics website (http://www.linkedomics.org/login.php). The survival of subjects was estimated by the Kaplan-Meier method and the difference was analyzed by Log-rank test. All statistical analyses were performed using GraphPad Prism 5. A two-tailed *P*-value of <0.05 was considered statistically significant.

Results

TFT selectively inhibits the proliferation of TNBC cells

To identify small molecular drug(s) with anticancer activity against TNBC cells, we used MTT assays to screen individual drugs in the FDA-approved drug library in MDA-MB-231 cells. We identified gemicitabine and trifluridine with cytotoxicity against MDA-MB-231 cells in vitro (**Figure 1A**). Because gemicitabine has been used as anticancer drugs in the clinic, we focused on the effect of TFT on the growth of TNBC in vitro and in vivo. To determine the antitumor activity of TFT, breast cancer MCF-7, MDA-MB-231, BT-549, Hs578T and control non-tumor MCF-10A cells were treated with different concentrations of TFT (5-20 μM) of TFT for 24-72 h. The cell viability was determined by MTT and cell counting. As shown in **Figure 1B** and **1C**, treatment with TFT did not affect the viability of MCF7 and MCF-10A cells, and the same treatment significantly reduced the viability of all TNBC cells in a dose- and time-dependent manner. Flow cytometry analysis indicated that treatment with 10 or 20 μM TFT significantly inhibited the proliferation of MDA-MB-231, BT549 and Hs578T cells, but not MCF-7 and MCF-10A cells and the inhibitory effects of different doses of TFT on TNBC cell proliferation tended to be dose-dependent (**Figure 1D**).

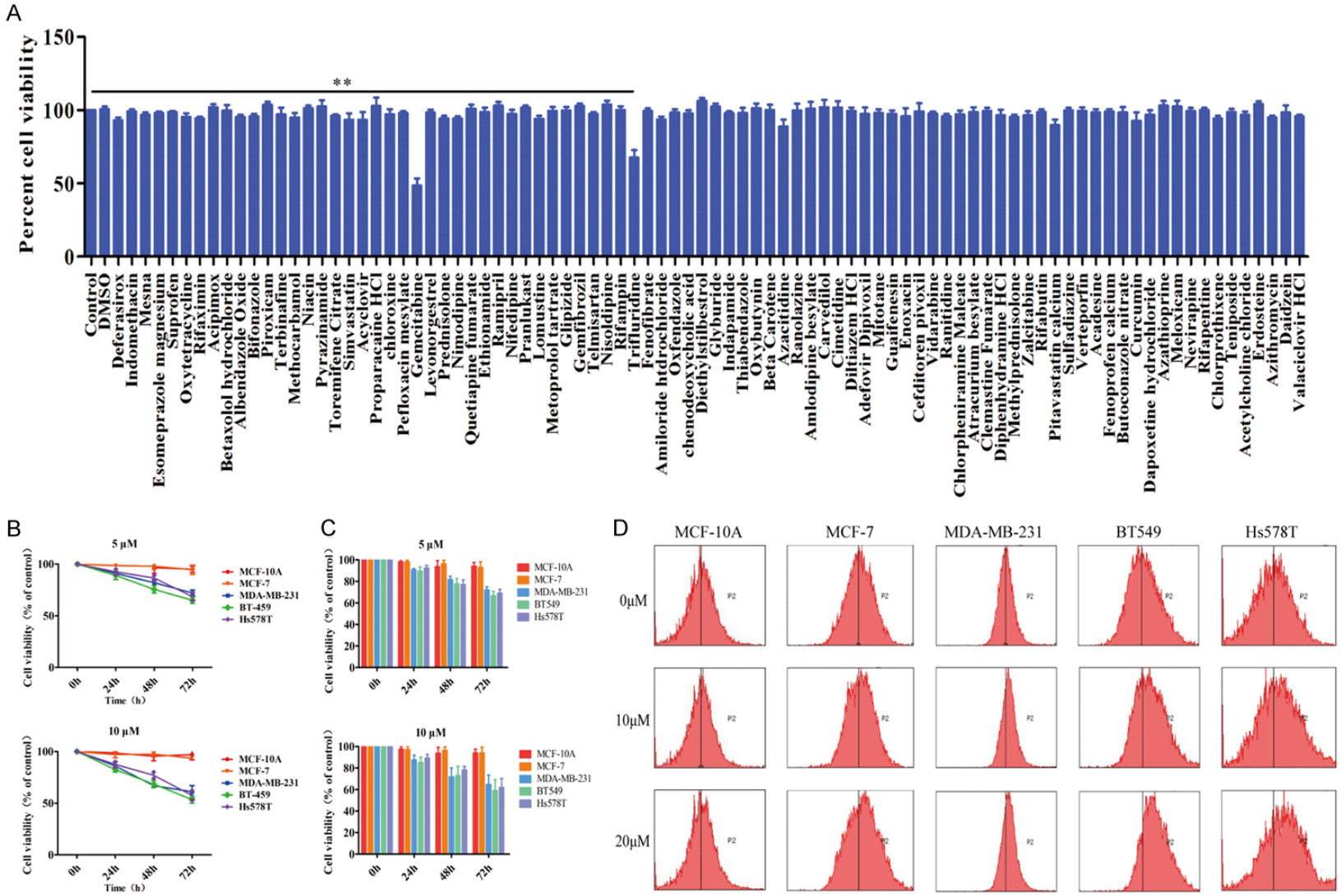
A
Percent cell viability
150
100
50
0
**
Control
DMSO
Deferasirox
Indomethacin
Mesna
Esomeprazole magnesium
Suprofen
Oxytetracycline
Rifaximin
Acipimox
Betaxolol hydrochloride
Albendazole Oxide
Bifonazole
Piroxicam
Terbinafine
Methocarbamol
Niacin
Pyrazinamide
Toremifene Citrate
Simvastatin
Acyclovir
Proparacaine HCl
chloroxine
Pefloxacin mesylate
Gemcitabine
Levonorgestrel
Prednisolone
Nimodipine
Quetiapine fumarate
Ethionamide
Ramipril
Nifedipine
Pranlukast
Lomustine
Metoprolol tartrate
Glipizide
Gemfibrozil
Telmisartan
Nisoldipine
Rifampin
Trifluridine
Fenofibrate
Amiloride htdrochloride
Oxfendazole
chenodeoxycholic acid
Diethylstilbestrol
Glyburide
Indapamide
Thiabendazole
Oxybutynin
Beta Carotene
Azacitidine
Ranolazine
Amlodipine besylate
Carvedilol
Cimetidine
Diltiazem HCl
Adefovir Dipivoxil
Mitotane
Guaifenesin
Enoxacin
Cefditoren pivoxil
Vidarabine
Ranitidine
Chlorpheniramine Maleate
Atracurium besylate
Clemastine Fumarate
Diphenhydramine HCl
Methylprednisolone
Zalcitabine
Rifabutin
Pitavastatin calcium
Sulfadiazine
Verteporfin
Acadesine
Fenoprofen calcium
Butoconazole nitrate
Curcumin
Dapoxetine hydrochloride
Azathioprine
Meloxicam
Nevirapine
Rifapentine
Chlorprothixene
Teniposide
Acetylcholine chloride
Erdosteine
Azithromycin
Daidzein
Valaciclovir HCl
B
5 μM
10 μM
Cell viability (% of control)
Time (h)
0h
24h
48h
72h
MCF-10A
MCF-7
MDA-MB-231
BT-459
Hs578T
C
5 μM
10 μM
Cell viability (% of control)
MCF-10A
MCF-7
MDA-MB-231
BT549
Hs578T
D
MCF-10A
MCF-7
MDA-MB-231
BT549
Hs578T
0μM
10μM
20μM
P2

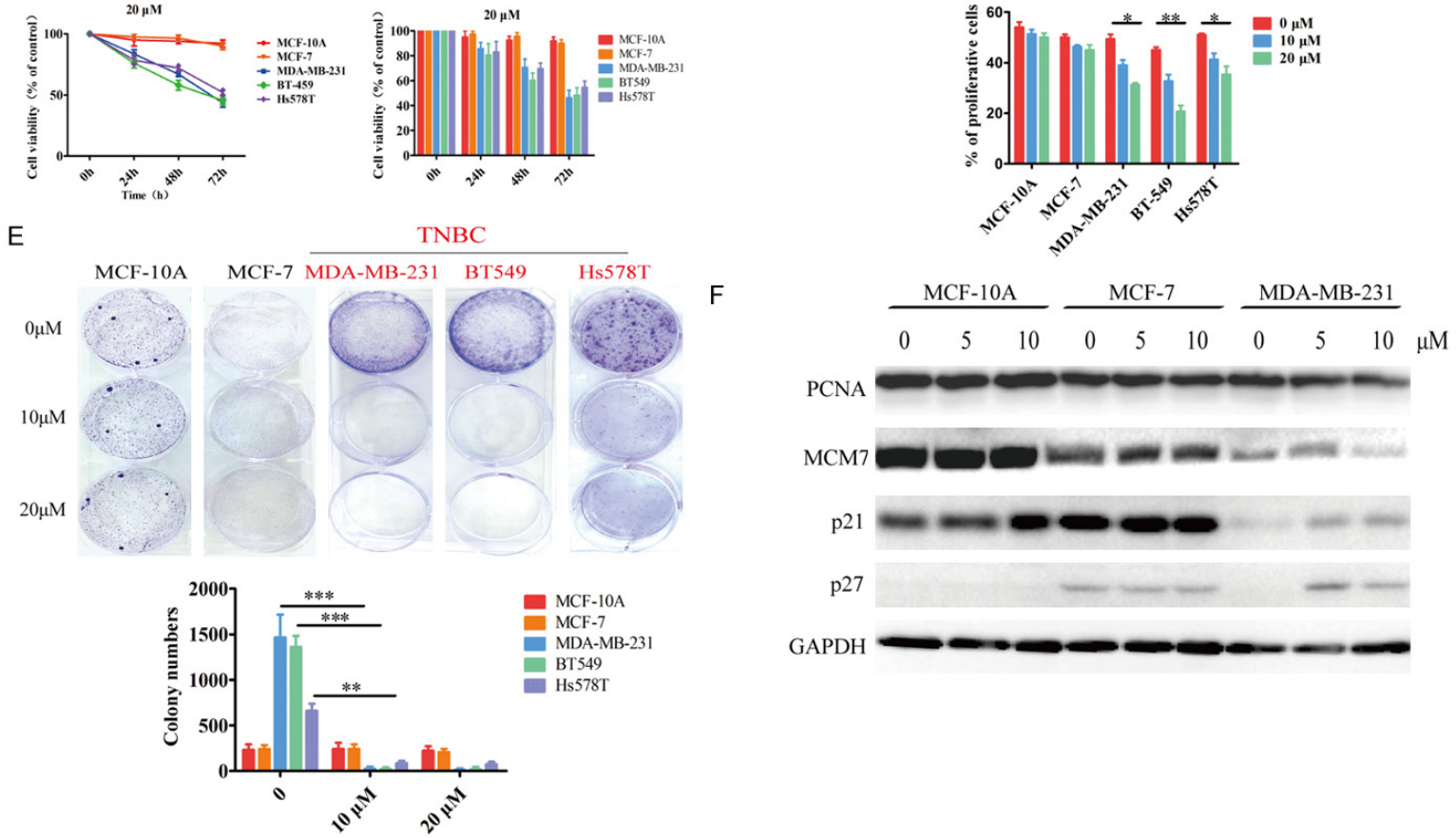

Figure 1. TFT selectively inhibits the proliferation of TNBC cells in vitro. (A) MDA-MB-231 cells were treated in triplicate with, or without, (control), vehicle DMSO, each indicated drug for 48 hours and the cell viability was assayed. (B) MCF-10A, MCF-7, MDA-MB-231, BT-549 and Hs578T cells were treated in triplicate with vehicle (control) or the indicated doses of TFT and their cell viability was measured by MTT or counted (C). (D) Flow cytometry analysis of proliferative cells after labeled with CFSE. (E) TFT inhibits the clonogenicity of TNBC cells. (F) Immunoblot analysis of cell proliferative regulators. Data are representative images, flow cytometry histograms or expressed as the mean ± SEM of each group of cells from three separate experiments. **P*<0.05, ***P*<0.01, ****P*<0.001 vs. the control.

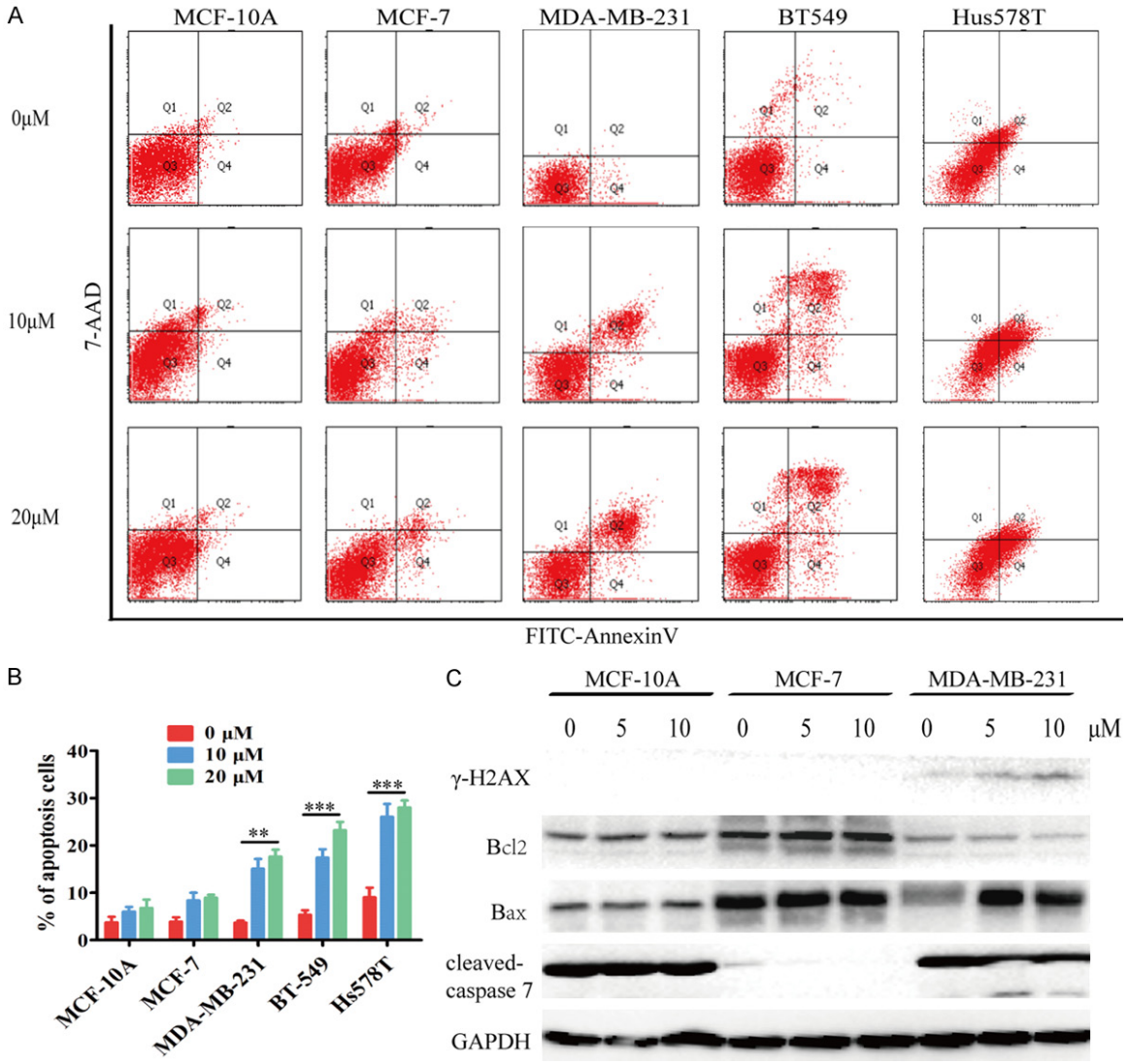

Figure 2. TFT induces the apoptosis of TNBC cells. MCF-10A, MCF-7, MDA-MB-231, BT-549 and Hs578T cells were treated in triplicate with vehicle (control) or the indicated doses of TFT for 48 h. A. The percentages of apoptotic cells were determined by flow cytometry. B. Statistical analysis of the frequency of apoptotic cells. C. Immunoblot analysis of the relative expression levels of apoptotic regulators. Data are representative flow cytometry charts, images or expressed as the mean ± SEM of each group of cells. ***P*<0.01, ****P*<0.001 vs. the control.

Further colony formation assays revealed that treatment with 10 or 20 μM TFT demolished the colony formation of MDA-MB-231, BT549 and Hs578T cells, but not MCF-7 and MCF-10A cells (**Figure 1E**). Because inhibition on cell proliferation usually is associated with the imbalance in the expression levels of cell cycle regulators, we examined the expression of proliferating cell nuclear antigen (PCNA), minichromosome maintenance component 7 (MCM7) and the S phase inhibitor p21 and p27 by immunoblot assays. The results displayed that treatment with 5 or 10 μM TFT decreased the levels of S phase proteins PCNA and replication licensing factor MCM7 expression, and increased G1 phase inhibitors p21 and p27 expression in MDA-MB-231 cells (**Figure 1F**). However, the same treatment did not significantly alter the expression levels of these proteins in MCF-10A and MCF-7 cells. Collectively, such data demonstrated that treatment with TFT selectively inhibited the proliferation of TNBC cells in vitro.

TFT induces TNBC cell apoptosis

To understand how TFT inhibited TNBC cell proliferation, we determined the effect of TFT on TNBC cell apoptosis by flow cytometry. Treat-

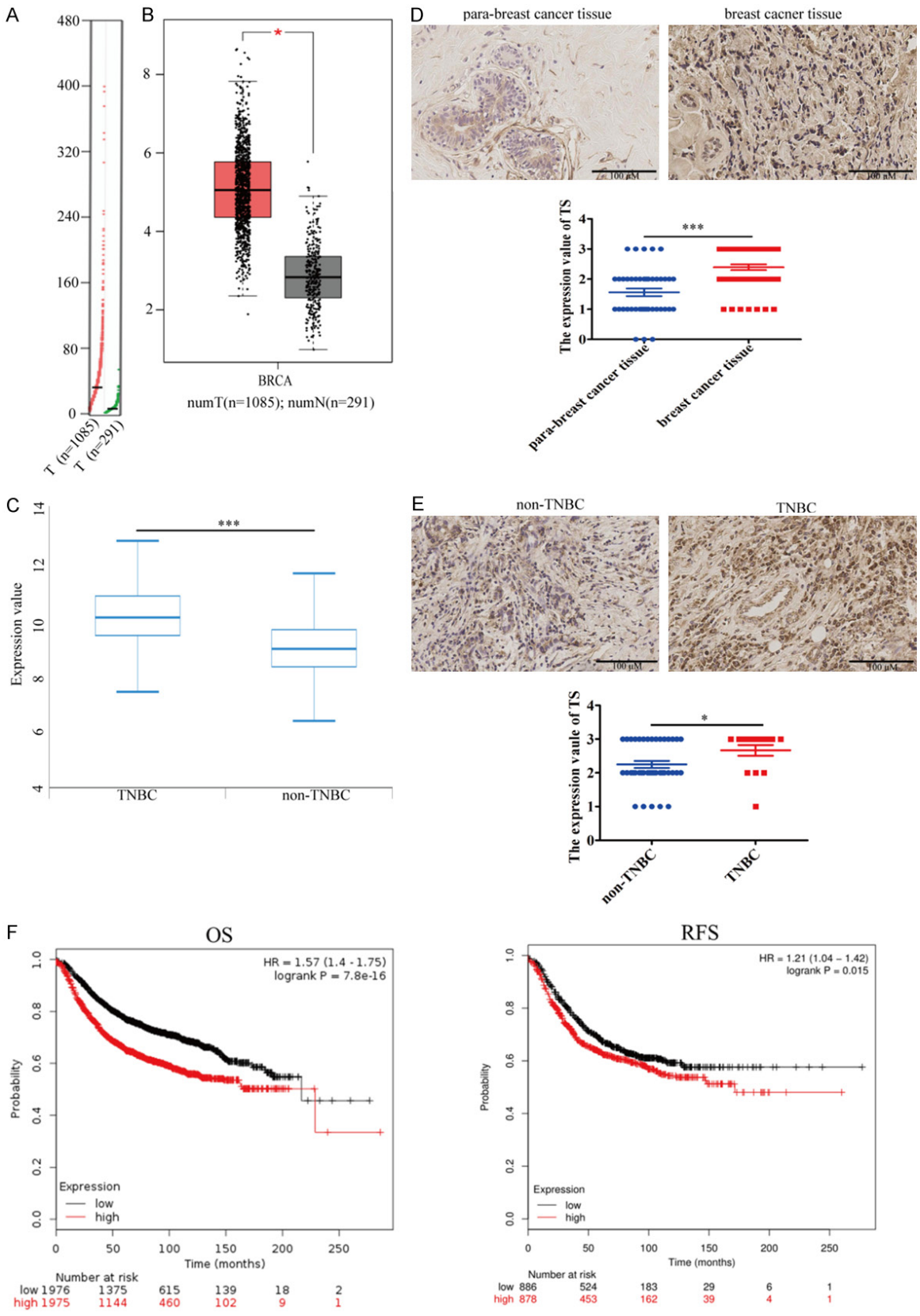

Figure 3. Upregulated TS expression is associated with poor prognosis in breast cancer. A, B. TS mRNA transcripts in 1085 breast cancer and 291 normal breast tissues in the GEPIA database. C. TS mRNA transcripts in 876 non-TNBC breast cancer and 193 TNBC breast tissues in the GEPIA database. D. Immunohistochemistry analysis of TS

expression in 56 breast cancer and 41 para-breast cancer tissues in a microtissue array. E. Immunohistochemistry analysis of TS expression in 15 TNBC and 41 non-TNBC breast cancer tissues array. F. Stratification analysis of overall survival and disease free survival curves of patients with high or lower TS-expressing breast cancers. Data are representative images, or expressed as the median ± IQR of each group of subjects. *P<0.05, ***P<0.001 vs. the control.

ment with 10 or 20 μM TFT significantly increased the percentages of apoptotic TNBC cells (**Figure 2A** and **2B**). Further immunoblot analysis revealed that treatment with 5 or 10 μM TFT increased pro-apoptotic γ-H2AX, Bax, cleaved caspase-7 expression, and decreased anti-apoptotic Bcl-2 expression in MDA-MB-231 cells, but not in MCF-10A and MCF-7 cells (**Figure 2C**). Such data indicated that TFT selectively induced TNBC cell apoptosis in vitro.

UP-regulated TS expression is associated with poor prognosis of TNBC

Previous studies have shown that TFT targets TS to inhibit cancer growth [16, 17] and up-regulated TS expression is associated with the proliferation and survival of lung, colon cancer and mesothelioma cells [10-12]. Next, we examined how TS expression could be associated with the progression of TNBC. We analyzed the expression levels of TS in normal breast tissue and breast cancer tissues in the GEPIA database. The results displayed that the relative levels of TS mRNA transcripts in breast cancer tissues were significantly higher than that in normal breast tissues (P<0.05, **Figure 3A** and **3B**). Furthermore, the relative levels of TS mRNA transcripts in TNBC tissues were significantly higher than that in other types of breast cancers (P<0.001, **Figure 3C**). Immunohistochemistry analysis of the microtissue array indicated that the levels of TS protein expression in breast cancer tissues were also significantly higher than that in the non-tumor para-breast tissues (P<0.001, **Figure 3D**) and TS protein expression in the TNBC tissues was significantly higher than that in the non-TNBC tissues (P<0.05, **Figure 3E**). Stratification analyses indicated that the expression of TS was significantly associated with negative ER and PR expression, but not with HER2 expression in breast cancer (Supplementary Figure 1). The high TS expression was significantly associated with a shorter overall survival (OS) and disease free survival (RFS) of breast cancer patients in the GEPIA database (**Figure 3F**). Thus, high TS expression was associated with poor prognosis of breast cancer.

TS silencing inhibits the proliferation of TNBC cells

To determine the role of TS in breast cancer, the expression of TS was detected in different types of cells by immunoblot. The relative levels of TS expression in TNBC cells were higher than that in MCF-10A and MCF-7 cells (**Figure 4A**). Immunoblot revealed that transfection of MCF-7, MDA-MB-231 and BT-549 cells with TS-specific siRNA, but not control scramble siRNA, significantly decreased TS expression (**Figure 4B**). MTT assays exhibited that TS silencing significantly reduced the proliferation of MDA-MB-231 and BT549 cells, but not MCF-7 cells (**Figure 4C**). Flow cytometry analysis revealed that TS silencing selectively decreased the proliferation of TNBC cells (**Figure 4D** and **4E**), but did not significantly alter the frequency of apoptotic TNBC cells (**Figure 4F** and **4G**). Immunoblot analysis displayed that TS silencing decreased MCM7 and PCNA expression, and increased p21 and p27 expression in TNBC cells, but not in MCF-7 cells (**Figure 4H**). To test the inhibitory effect of TS silencing on the growth of TNBC in vivo, MDA-MB-231 cells were transduced with control lentivirus or lentivirus for the expression of TS-specific shRNA to establish a stably TS-silencing MDA-MB-231/shTS or MDA-MB-231/shCon cell line. Following implantation of NOD/scid mice with these cells for 21 days, we observed that TS silencing reduced the tumor sizes and weights in mice (**Figure 4I** and **4J**). Together, such data demonstrated that TS silencing selectively inhibited the proliferation of TNBC cells.

TFT induces DNA DSB in TNBC cells

Given that the results of TFT treatment and TS silencing to induce TNBC cell apoptosis were controversial and aberrant DSB is associated with cell apoptosis [18, 19], we tested the effect of TFT on DSB in different types of cells by immunofluorescent analysis of γ-H2AX expression. We observed that treatment with TFT resulted in fragmented anti-γ-H2AX staining in the nuclei of MDA-MB-231 and BT-549 cells, but only little or no anti-γ-H2AX staining in

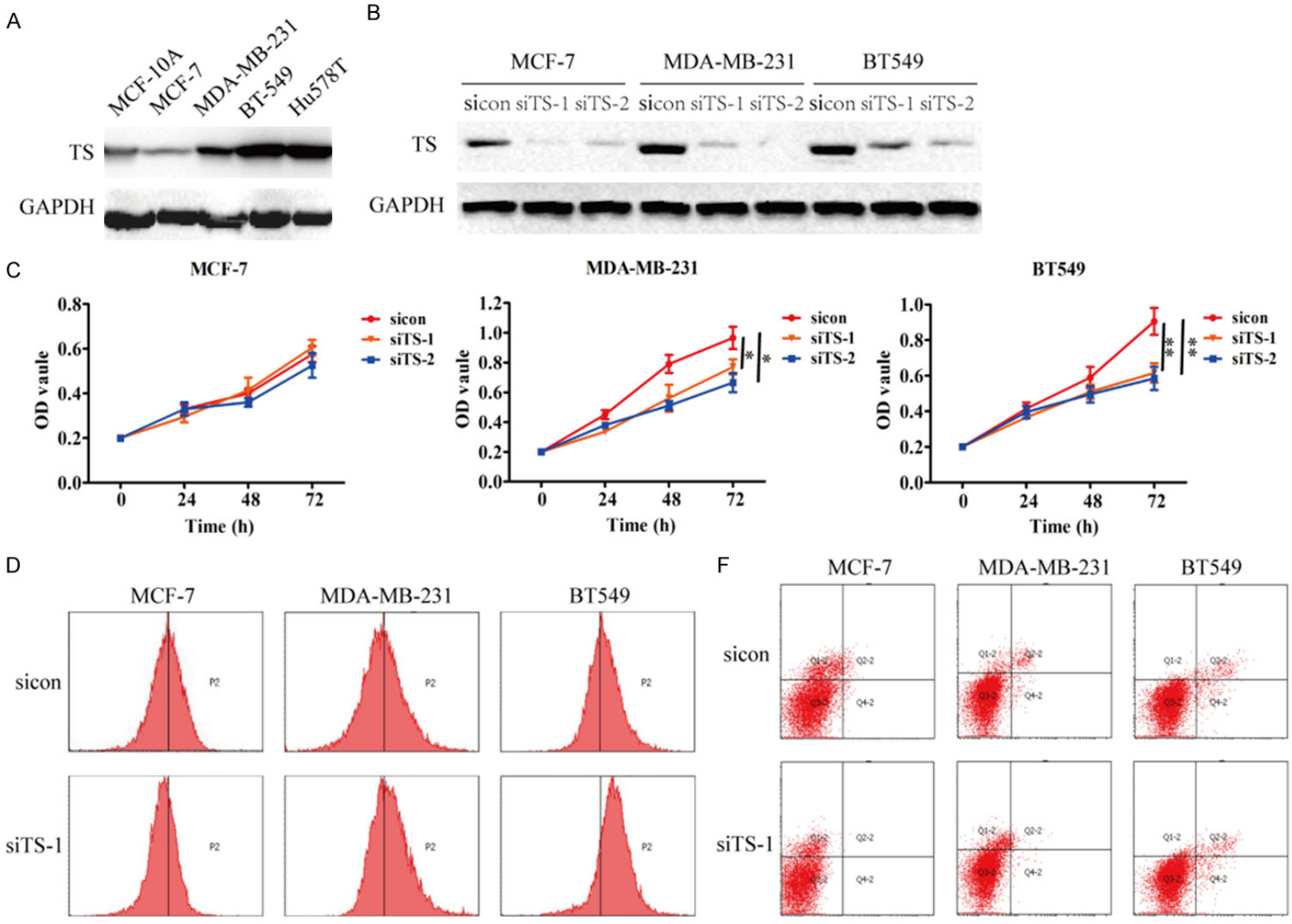
A
MCF-10A
MCF-7
MDA-MB-231
BT-549
Hu578T
TS
GAPDH
B
MCF-7
MDA-MB-231
BT549
sicon siTS-1 siTS-2 sicon siTS-1 siTS-2 sicon siTS-1 siTS-2
TS
GAPDH
C
MCF-7
MDA-MB-231
BT549
OD vaule
Time (h)
sicon
siTS-1
siTS-2
D
MCF-7
MDA-MB-231
BT549
sicon
siTS-1
P2
F
MCF-7
MDA-MB-231
BT549
sicon
siTS-1

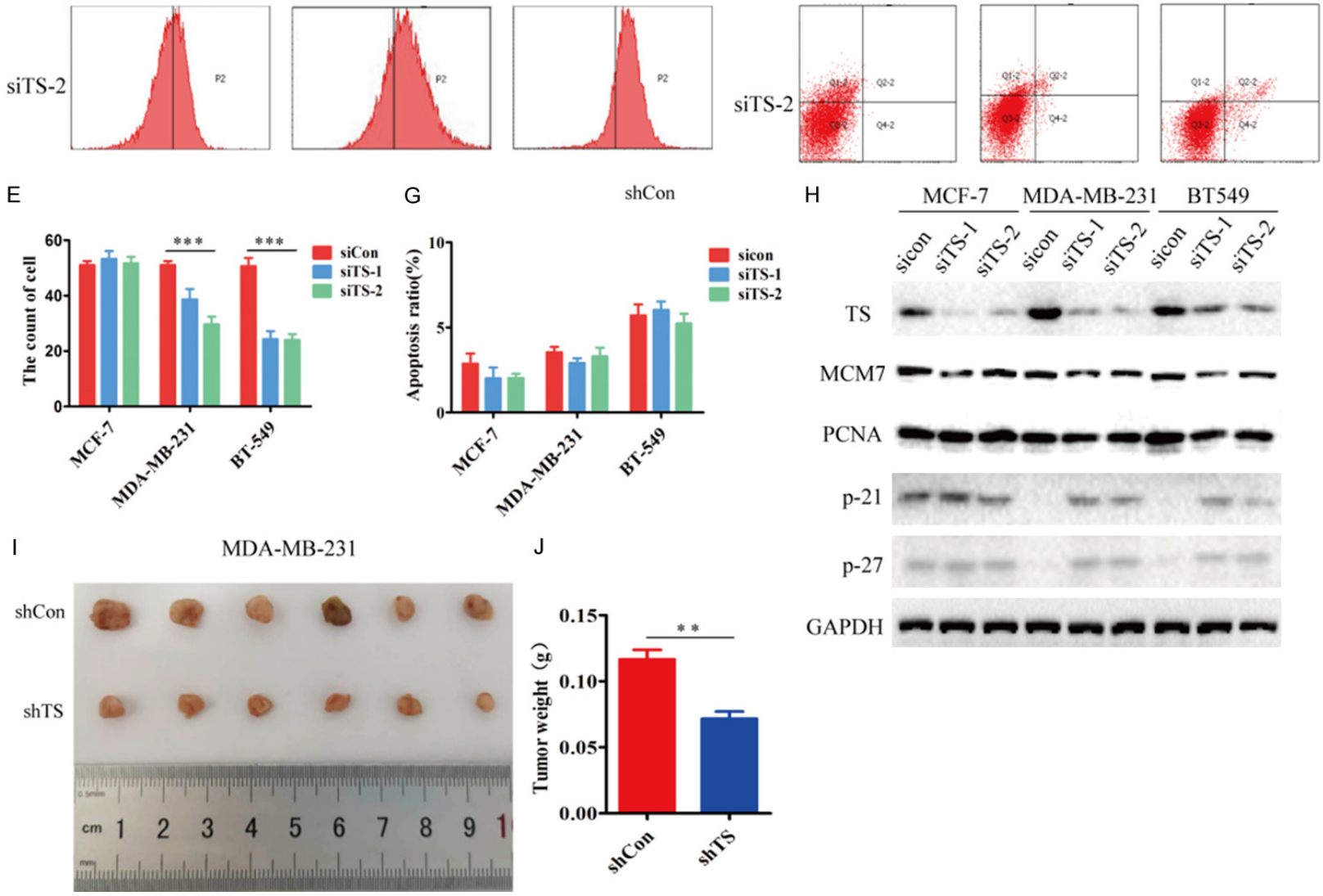

Figure 4. TS silencing inhibits the proliferation of TNBC cells. A. Immunoblot analysis of TS expression in MCF-10A, MCF-7, MDA-MB-231, BT-549 and Hs578T cells. B. TS silencing in the indicated cells. C. TS silencing reduces the viability of TNBC cells. D-G. Flow cytometry analysis of the effect of TS silencing on the proliferation and apoptosis of breast cancer cells. H. Immunoblot analysis of the relative expression levels of cell cycle regulators. I. Female NOD/scid mice were implanted with MDA-MB-231/shCon and MDA-MB-231/shTS cells, respectively. At the end of the experiment, their tumors were dissected and photoimaged. J. The tumor weights were measured. Data are representative images, or expressed as the mean ± SEM of each group of cells from three separate experiments. *P<0.05, **P<0.01, ***P<0.001 vs. the control.

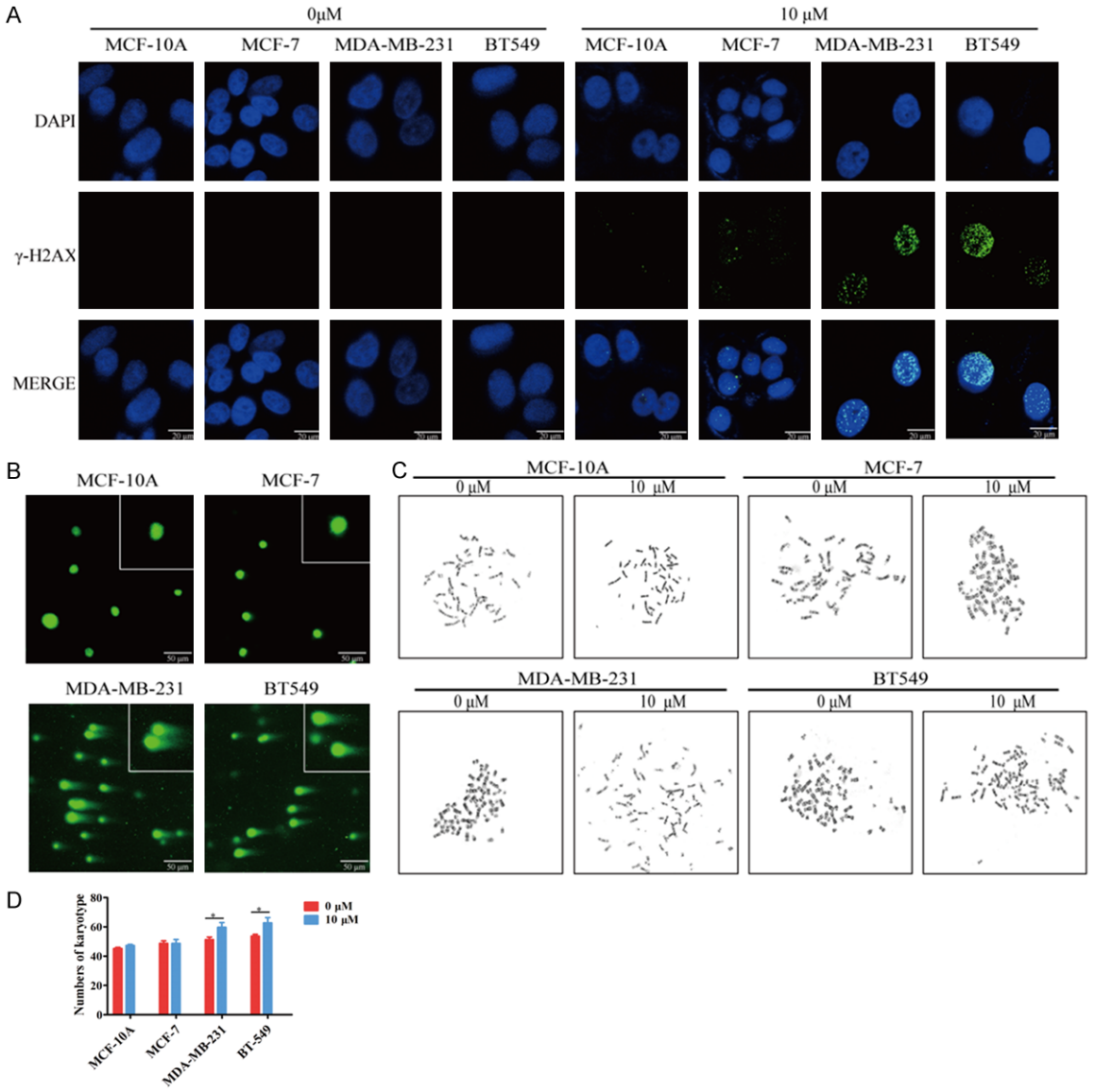

Figure 5. TFT induces DNA double-strand break in TNBC cells. A. MCF-10A, MCF-7, MDA-MB-231 and BT-549 were treated in triplicate with vehicle or TFT (10 μM) for 72 h. The γ-H2AX expression was analyzed by immunofluorescence. B. The comet assay analysis of karyotype chromosomes in different groups of cells. C. Chromosomal instability was examined using a chromosome karyotype analyzer. D. Statistical analysis of the number of chromosome karyotype. Data are representative images, or expressed as the mean ± SEM of each group of cells. **P*<0.05 vs. the control.

MCF-10A and MCF-7 (**Figure 5A**). Alkaline comet assays revealed that treatment with TFT led to more DNA damages in MDA-MB-231 and BT-549 cells than in MCF-10A and MCF-7 cells (**Figure 5B**). Further karyotype analysis revealed that treatment with TFT selectively increased the number of chromosomes in karyotype of MDA-MB-231 and BT-549 cells (**Figure 5C** and **5D**). Therefore, treatment with TFT resulted in chromosome instability and damages, associated with its pro-apoptotic effect in TNBC cells.

Treatment with TFT inhibits the growth of implanted mouse TNBC tumors in vivo

Finally, we investigated whether treatment with TFT could inhibit mouse TNBC growth in vivo. Individual BALB/C mice were implanted with mouse TNBC 4T1 cells into their fat pad and when the establishment of solid tumors, the mice were randomized and treated orally with vehicle, 75 or 150 mg/kg TFT daily. We found that treatment with TFT significantly inhibited

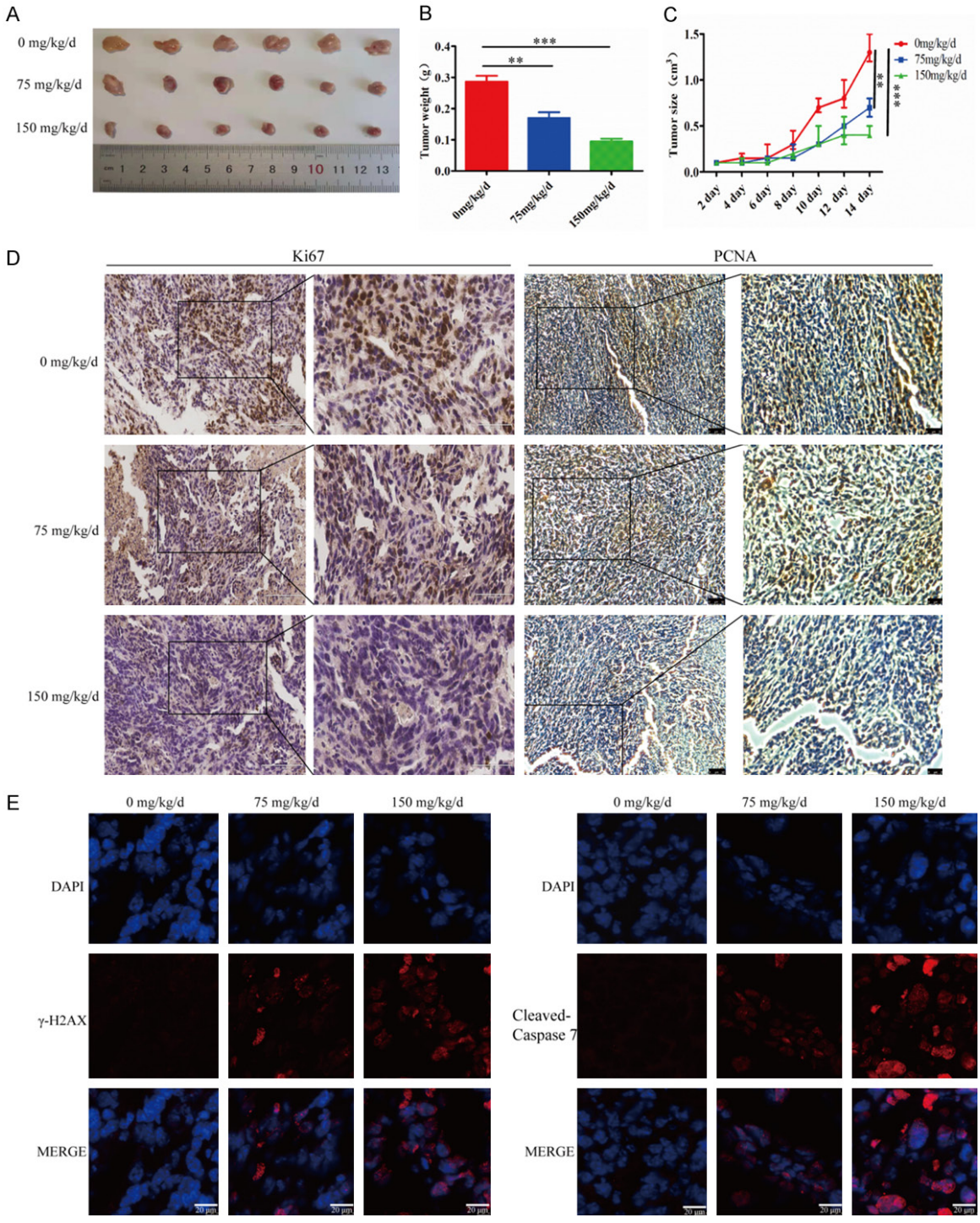

Figure 6. TFT treatment significantly inhibits the growth of mouse TNBC tumors in vivo. Female BALB/c mice were injected with 4T1 cells to establish TNBC tumors. The mice were randomized and treated with vehicle, 75 mg/kg/day or 150 mg/kg/day of TFT by gavage daily for 10 days. A. The dynamic growth of TNBC tumors. B. Tumor weights. C. Photoimaging tumor sizes. D. Immunohistochemistry analysis of Ki67 and MCM7 expression in tumors tissues. E. Immunofluorescent analysis of anti-γ-H2AX and anti-cleaved-caspase 7 signals in tumor tissues. Data are representative images, or expressed as the mean ± SEM of each group of cells. $^{**}P<0.01$, $^{***}P<0.001$ vs. the control.

the growth of implanted TNBC and the inhibitory effects of two doses of TFT treatment on the growth of mouse TNBC trended to be dose-dependent (**Figure 6A**). Treatment with TFT

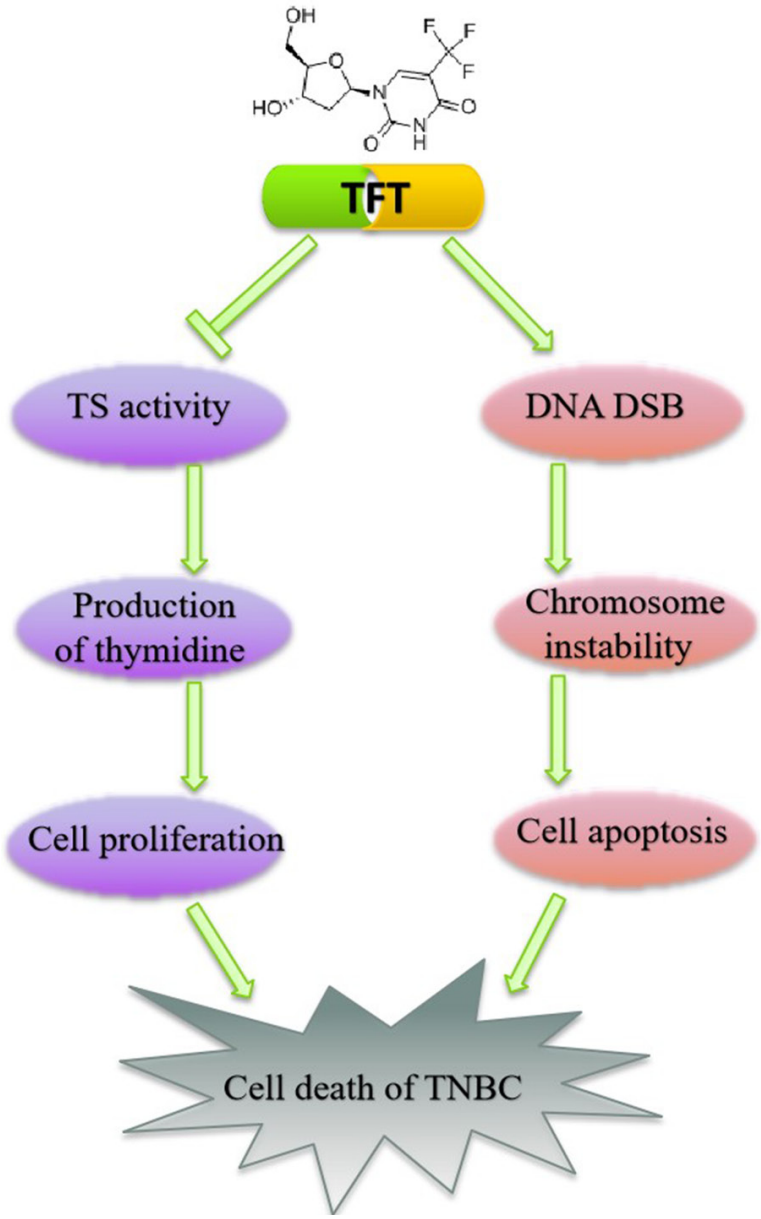

Figure 7. Schematic model.

obviously reduced the tumor weights and sizes (**Figure 6B** and **6C**). Immunohistochemistry indicated that the levels of Ki67 and PCNA protein expression in the TFT-treated tumors were lower than that in the control (**Figure 6D**). Immunofluorescent assays revealed that anti-γ-H2AX and anti-cleaved caspase-7 fluorescent signals in the TFT-treated tumors were higher than that in the control (**Figure 6E**). Collectively, treatment with TFT significantly inhibited the growth of implanted mouse TNBC in vivo, which was associated with inducing their apoptosis and inhibiting cell proliferation.

Discussion

TNBC is insensitive to common targeted therapies and depends on surgical resection and chemotherapies. However, TNBC has a high rate of recurrence, distant metastasis and drug resistance, leading to poor prognosis. TNBC patients are usually treated with anthracycline and taxane-based chemotherapies because TNBC usually express high levels of TS. TFT, like Fluorouracil (5-FU), can bind to TS to inhibit TS activity and incorporate into DNA, leading to DNA damage and cell death [7, 9, 20-23]. In this study, we found that treatment with TFT selectively inhibited the proliferation of TNBC cells in vitro and attenuated the growth of implanted TNBC tumors in vivo. Our data extended previous observations in colon, lung and prostatic cancer cells [10-12]. Given that TFT can inhibit the proliferation of 5-FU-resistant cancer cells [24, 25] our findings may aid in design of new chemotherapies for TNBC, particularly for TNBC refractory to 5-FU.

TS is crucial for thymidine and DNA synthesis, which promotes cell proliferation, particularly for rapid proliferative tumor cells [26, 27]. In our study, we found that TS expression was up-regulated in breast cancer, particularly in TNBC and high TS expression was significantly associated with shorter OS and RFS in breast cancer patients. Moreover, TS silencing selectively inhibited the proliferation of TNBC cells, accompanied by up-regulating p21 and p27 expression and down-regulating MCM7 and PCNA expression. Actually, treatment with capecitabine to target TS effectively inhibits the growth of TNBC patient-derived xenografts (PDX) [28] and inhibition of TS by Arsenic trioxide (ATO) attenuates the proliferation of lung and

colon adenocarcinoma cells [11, 12, 29]. Apparently, TS may be a therapeutic target for intervention of TNBC. Thus, our finding may aid in design of TS-specific therapies for TNBC. It is notable that while treatment with TFT triggered TNBC cell apoptosis while TS silencing failed to induce TNBC cell apoptosis. Furthermore, the inhibitory effect of TFT on the proliferation of TNBC cells was much stronger than that of TS silencing. Such data suggest that TFT may inhibit the proliferation of TNBC cells not only by inhibiting TS activity, but also by other unknown mechanisms. We are interested in further investigating the pharmacological action of TFT in inhibiting TNBC cell proliferation.

TFT can incorporate into DNA and induce DNA DSB [8, 23]. In this study, we found that treatment with TFT increased the number of DNA DBS and karyotype chromosomes in TNBC cells, accompanied by increased levels of γ-H2AX expression. Such data indicated that TFT treatment induced chromosome instability. There data were consistent with previous observations that TFT treatment incorporates in DNA and induces DAN fragmentation [8, 25, 30]. The increased chromosome instability and DNA fragmentation may contribute to the enhanced cell apoptosis of TNBC cells and may explain the stronger inhibitory effect of TFT on the proliferation of TNBC. Hence, our findings may provide new insights in the pharmacological action of TFT in inhibiting TNBC growth.

In conclusion, our data indicated that TFT effectively inhibited TNBC cell proliferation and induced TNBC cell apoptosis, which were associated with modulating the expression of cell cycle regulators and increasing DNA DSB and chromosome instability in TNBC cells (**Figure 7**). Therefore, TS may be a biomarker for prognosis and therapeutic target of TNBC and TFT may be a valuable candidate drug for the intervention of TNBC.

Acknowledgements

The project was funded by the grants from the National Natural Science Foundation of China (no. 81502620 and no. 81672810) and the First Affiliated Hospital of Xian Jiaotong University College of Medicine Foundation (no. 2018MS-03). The author disclaims that there is no conflict of interest in the study, authorship, and/or publication of this article.

Disclosure of conflict of interest

None.

Address correspondence to: Dr. Peijun Liu, Center for Translational Medicine, The First Affiliated Hospital of Xi'an Jiaotong University, 277 West Yanta Road, Xi'an 710061, Shaanxi, PR China. Tel: +86-18991232306; Fax: +86-029-85324628; E-mail: liupeijun@xjtu.edu.cn

References

[1] Bauer KR, Brown M, Cress RD, Parise CA and Caggiano V. Descriptive analysis of estrogen receptor (ER)-negative, progesterone receptor (PR)-negative, and HER2-negative invasive breast cancer, the so-called triple-negative phenotype: a population-based study from the California cancer Registry. Cancer 2007; 109: 1721-1728.

[2] Rakha EA, Elsheikh SE, Aleskandarany MA, Habashi HO, Green AR, Powe DG, El-Sayed ME, Benhasouna A, Brunet JS, Akslen LA, Evans AJ, Blamey R, Reis-Filho JS, Foulkes WD and Ellis IO. Triple-negative breast cancer: distinguishing between basal and nonbasal subtypes. Clin Cancer Res 2009; 15: 2302-2310.

[3] Gucalp A and Traina TA. Triple-negative breast cancer: adjuvant therapeutic options. Chemother Res Pract 2011; 2011: 696208.

[4] Dent R, Trudeau M, Pritchard KI, Hanna WM, Kahn HK, Sawka CA, Lickley LA, Rawlinson E, Sun P and Narod SA. Triple-negative breast cancer: clinical features and patterns of recurrence. Clin Cancer Res 2007; 13: 4429-4434.

[5] Carmine AA, Brogden RN, Heel RC, Speight TM and Avery GS. Trifluridine: a review of its antiviral activity and therapeutic use in the topical treatment of viral eye infections. Drugs 1982; 23: 329-353.

[6] Temmink OH, Comijn EM, Fukushima M and Peters GJ. Intracellular thymidylate synthase inhibition by trifluorothymidine in FM3A cells. Nucleosides Nucleotides Nucleic Acids 2004; 23: 1491-1494.

[7] Eckstein JW, Foster PG, Finer-Moore J, Wataya Y and Santi DV. Mechanism-based inhibition of thymidylate synthase by 5-(trifluoromethyl)-2'-deoxyuridine 5'-monophosphate. Biochemistry 1994; 33: 15086-15094.

[8] Emura T, Suzuki N, Yamaguchi M, Ohshimo H and Fukushima M. A novel combination antimetabolite, TAS-102, exhibits antitumor activity in FU-resistant human cancer cells through a mechanism involving FTD incorporation in DNA. Int J Oncol 2004; 25: 571-578.

[9] Temmink OH, Hoebe EK, van der Born K, Ackland SP, Fukushima M and Peters GJ. Mecha-

nism of trifluorothymidine potentiation of oxaliplatin-induced cytotoxicity to colorectal cancer cells. Br J Cancer 2007; 96: 231-240.
[10] Abu Lila AS, Moriyoshi N, Fukushima M, Huang CL, Wada H and Ishida T. Metronomic S-1 dosing and thymidylate synthase silencing have synergistic antitumor efficacy in a colorectal cancer xenograft model. Cancer Lett 2017; 400: 223-231.
[11] Lam SK, Mak JC, Zheng CY, Li YY, Kwong YL and Ho JC. Downregulation of thymidylate synthase with arsenic trioxide in lung adenocarcinoma. Int J Oncol 2014; 44: 2093-2102.
[12] Lam SK, Li YY, Zheng CY and Ho JC. Downregulation of thymidylate synthase and E2F1 by arsenic trioxide in mesothelioma. Int J Oncol 2015; 46: 113-122.
[13] Temmink OH, Emura T, de Bruin M, Fukushima M and Peters GJ. Therapeutic potential of the dual-targeted TAS-102 formulation in the treatment of gastrointestinal malignancies. Cancer Sci 2007; 98: 779-789.
[14] Li J, Liu J, Liang Z, He F, Yang L, Li P, Jiang Y, Wang B, Zhou C, Wang Y, Ren Y, Yang J, Zhang J, Luo Z, Vaziri C and Liu P. Simvastatin and Atorvastatin inhibit DNA replication licensing factor MCM7 and effectively suppress RB-deficient tumors growth. Cell Death Dis 2017; 8: e2673.
[15] Ford CE, Ekstrom EJ and Anderson T. Retraction for Ford et al., Wnt-5a signaling restores tamoxifen sensitivity in estrogen receptor-negative breast cancer cells. Proc Natl Acad Sci U S A 2010; 107: 22360.
[16] Reyes P and Heidelberger C. Fluorinated pyrimidines. XXVI. Mammalian thymidylate synthetase: its mechanism of action and inhibition by fluorinated nucleotides. Mol Pharmacol 1965; 1: 14-30.
[17] Fujiwara Y, Oki T and Heidelberger C. Fluorinated pyrimidines. XXXVII. Effects of 5-trifluoromethyl-2'-deoxyuridine on the synthesis of deoxyribonucleic acid of mammalian cells in culture. Mol Pharmacol 1970; 6: 273-280.
[18] Cook PJ, Ju BG, Telese F, Wang X, Glass CK and Rosenfeld MG. Tyrosine dephosphorylation of H2AX modulates apoptosis and survival decisions. Nature 2009; 458: 591-596.
[19] Banath JP, Klokov D, MacPhail SH, Banuelos CA and Olive PL. Residual gammaH2AX foci as an indication of lethal DNA lesions. BMC Cancer 2010; 10: 4.
[20] Pinedo HM and Peters GF. Fluorouracil: biochemistry and pharmacology. J Clin Oncol 1988; 6: 1653-1664.
[21] Santi DV and Sakai TT. Thymidylate synthetase. Model studies of inhibition by 5-trifluoromethyl-2'-deoxyuridylic acid. Biochemistry 1971; 10: 3598-3607.
[22] Temmink OH, de Bruin M, Comijn EM, Fukushima M and Peters GJ. Determinants of trifluorothymidine sensitivity and metabolism in colon and lung cancer cells. Anticancer Drugs 2005; 16: 285-292.
[23] Emura T, Nakagawa F, Fujioka A, Ohshimo H, Yokogawa T, Okabe H and Kitazato K. An optimal dosing schedule for a novel combination antimetabolite, TAS-102, based on its intracellular metabolism and its incorporation into DNA. Int J Mol Med 2004; 13: 249-255.
[24] Overman MJ, Varadhachary G, Kopetz S, Thomas MB, Fukushima M, Kuwata K, Mita A, Wolff RA, Hoff PM, Xiong H and Abbruzzese JL. Phase 1 study of TAS-102 administered once daily on a 5-day-per-week schedule in patients with solid tumors. Invest New Drugs 2008; 26: 445-454.
[25] Emura T, Murakami Y, Nakagawa F, Fukushima M and Kitazato K. A novel antimetabolite, TAS-102 retains its effect on FU-related resistant cancer cells. Int J Mol Med 2004; 13: 545-549.
[26] Lane AN and Fan TW. Regulation of mammalian nucleotide metabolism and biosynthesis. Nucleic Acids Res 2015; 43: 2466-2485.
[27] Tong X, Zhao F and Thompson CB. The molecular determinants of de novo nucleotide biosynthesis in cancer cells. Curr Opin Genet Dev 2009; 19: 32-37.
[28] Marangoni E, Laurent C, Coussy F, El-Botty R, Chateau-Joubert S, Servely JL, de Plater L, Assayag F, Dahmani A, Montaudon E, Nemati F, Fleury J, Vacher S, Gentien D, Rapinat A, Foidart P, Sounni NE, Noel A, Vincent-Salomon A, Lae M, Decaudin D, Roman-Roman S, Bieche I, Piccart M and Reyal F. Capecitabine efficacy is correlated with TYMP and RB1 expression in PDX established from triple-negative breast cancers. Clin Cancer Res 2018; 24: 2605-2615.
[29] Lam SK, Li YY, Zheng CY, Leung LL and Ho JC. E2F1 downregulation by arsenic trioxide in lung adenocarcinoma. Int J Oncol 2014; 45: 2033-2043.
[30] Suzuki N, Nakagawa F, Nukatsuka M and Fukushima M. Trifluorothymidine exhibits potent antitumor activity via the induction of DNA double-strand breaks. Exp Ther Med 2011; 2: 393-397.

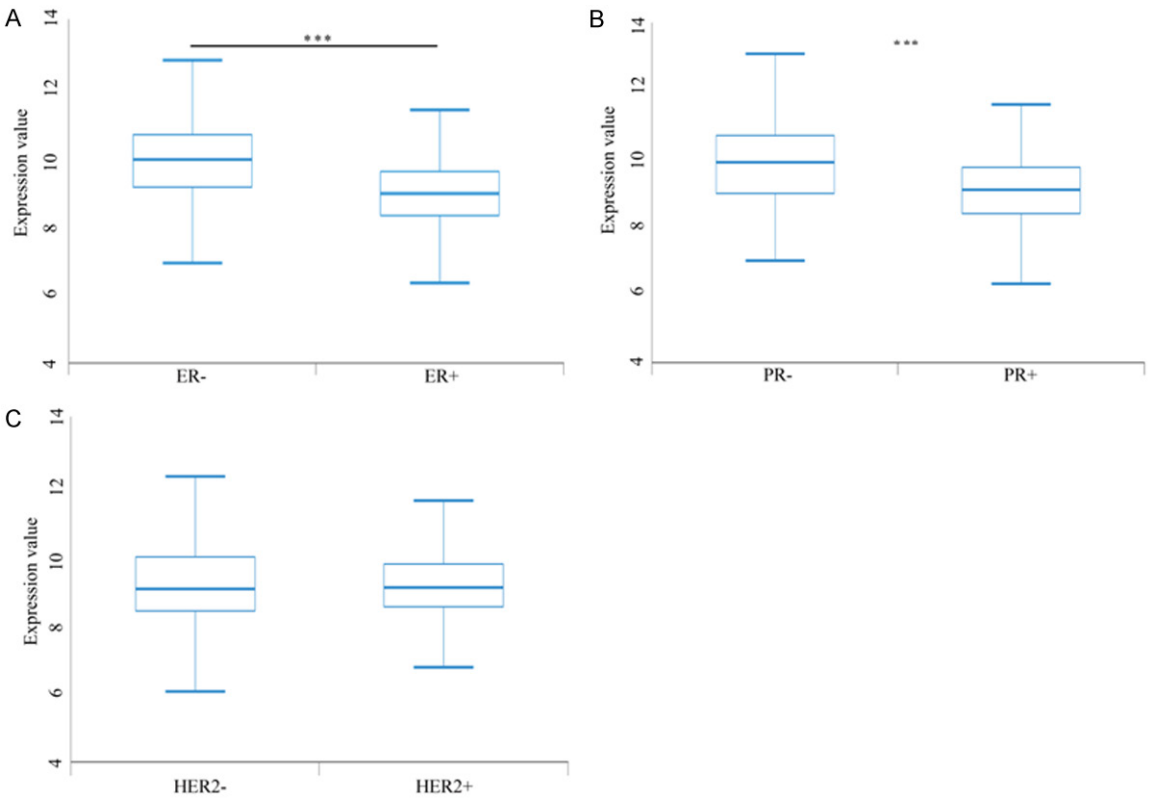

Supplementary Figure 1. TS mRNA transcripts in ER+ and ER- (A), PR+ and PR- (B), HER2+ and HER2- (C) breast cancers in the GEPIA database. ***P<0.001 vs. the control.